

## Conservation Laws and Transport in Hamiltonian Chaos

F. Skiff, F. Andereg, T. N. Good, P. J. Paris, M. Q. Tran, N. Rynn,<sup>(a)</sup> and R. A. Stern<sup>(b)</sup>

*Centre de Recherches en Physique des Plasmas, Association Euratom - Confédération Suisse, Ecole Polytechnique Fédérale de Lausanne, 21, Av. des Bains, CH-1007 Lausanne, Switzerland*

(Received 11 April 1988)

Experiments are presented which demonstrate the conservation of certain integrals of motion during Hamiltonian chaos where the conservation of some of the integrals has been broken by the overlap of resonances. Experimentally, conservation laws are demonstrated through the observation of restrictions on transport, in phase space, of chaotic trajectories. Transport of plasma ions during stochastic motion in an electrostatic wave is followed by means of laser-induced fluorescence on metastable "test particles" produced by optical pumping.

PACS numbers: 05.45.+b, 52.25.Fi

Chaos, in classical Hamiltonian systems, is a reversible process. However, it is also true that intrinsic stochasticity may resemble a classical stochastic process under certain circumstances.<sup>1</sup> In plasma wave-particle interactions, phase decorrelation between a particle and wave frequently result in very similar particle energy gains (in the plasma frame) whether the decorrelation is brought about by an intrinsic or extrinsic (e.g., collisional) process. This similarity is even closer if an average is taken over an ensemble of particle initial conditions. Nevertheless, intrinsic stochasticity can be distinguished by a threshold, by a fast time scale, and by details in the particle distribution function.<sup>2</sup> In addition, a Hamiltonian description of wave-particle interaction generally contains symmetries (conservation laws) which would not be

present for a competing classically stochastic process. However, because of the inevitable self-consistent effects of chaotic particles on the plasma waves, it is not evident *a priori* that the Hamiltonian picture of single-particle motion should correctly predict the wave-induced transport above the stochasticity threshold. This Letter presents measurements of ion motion in phase space, during stochastic interaction with an electrostatic wave, which suggest the conservation of three integrals of the motion. Of the six integrals which exist for low wave amplitudes, three are no longer conserved when the wave amplitude is sufficient for "resonance overlap."

The Hamiltonian of specific interest to the interaction of a magnetized particle with an electrostatic wave has been given by Smith and Kaufman,<sup>3</sup>

$$H = P_z^2/2m + P_\theta \Omega + e\Phi_0 \cos[k_{\parallel}Z + k_{\perp}R - k_{\perp}\rho \sin(\phi + \theta)], \quad (1)$$

where  $\Omega$  is the gyrotron frequency and, in contrast to Ref. 3, we are considering a cylindrical wave. The definition of canonical variables is the same as in Ref. 3 [( $Z, P_z$ ) and ( $\phi, P_\phi = \frac{1}{2} m \Omega \rho^2$ )] with the addition of the cylindrical variables  $R = (X^2 + Y^2)^{1/2}$  and  $\theta = \tan^{-1}(X/Y)$  to replace the Cartesian coordinates  $X, Y$  of the guiding center. This is a canonical transformation between the old canonical variables ( $Y, m \Omega X$ ) and the new variables ( $\theta, P_\theta = \frac{1}{2} m \Omega R^2$ ).

Immediately it can be seen that  $H$  itself is a constant of the motion because  $\partial H / \partial t = 0$ . This means that the particle energy is constant in a frame of reference moving with the wave along the magnetic field [Eq. (1) is expressed in this frame]. In addition, it is evident that  $\partial H / \partial \phi = \partial H / \partial \theta$ . This is because the wave form is circularly symmetric. The particle angular momentum about the wave axis  $\frac{1}{2} m \Omega (R^2 - \rho^2)$  is therefore conserved. So long as  $\rho \ll R$ , i.e., the Larmor radius is small compared to the radial coordinate of the guiding center, then  $R$  will be constant during the motion. From the canonical equation for  $\theta$ ,

$$\partial \theta / \partial t = (k_{\perp} / k_{\parallel}) (m \Omega R)^{-1} \partial P_z / \partial t, \quad (2)$$

we see that, in the same limit ( $R$  constant), the motion of the guiding center in the  $\theta$  direction is linked to the acceleration along the magnetic field. Stated otherwise, the symmetries of the wave-particle Hamiltonian will restrict (for  $\rho \ll R$ ) motion of the particle guiding center to the  $\hat{\mathbf{E}} \times \hat{\mathbf{B}} = \hat{\theta}$  direction, and link this motion to changes in the parallel momentum.

Integration of the dynamical equations which follow from the Hamiltonian [Eq. (1)] indicates the conservation laws clearly. Figure 1 shows results from this integration. The three pairs of frames in Fig. 1 are Poincaré section plots (see Ref. 3) demonstrating the behavior of particle orbits both below [Figs. 1(a), 1(c), and 1(e)] and above [Figs. 1(b), 1(d), and 1(f)] the threshold for stochastic motion. Below threshold, subsequent intersections of particle orbits with the plane of section are very close to the initial conditions and indicate regular motion. In Fig. 1(c) a series of particles have been started along a vertical chord (in real space) which is normal to  $\mathbf{B}$ . This is done for the purpose of comparison with the experiment. The circle indicates the symmetry axis of the wave fields.

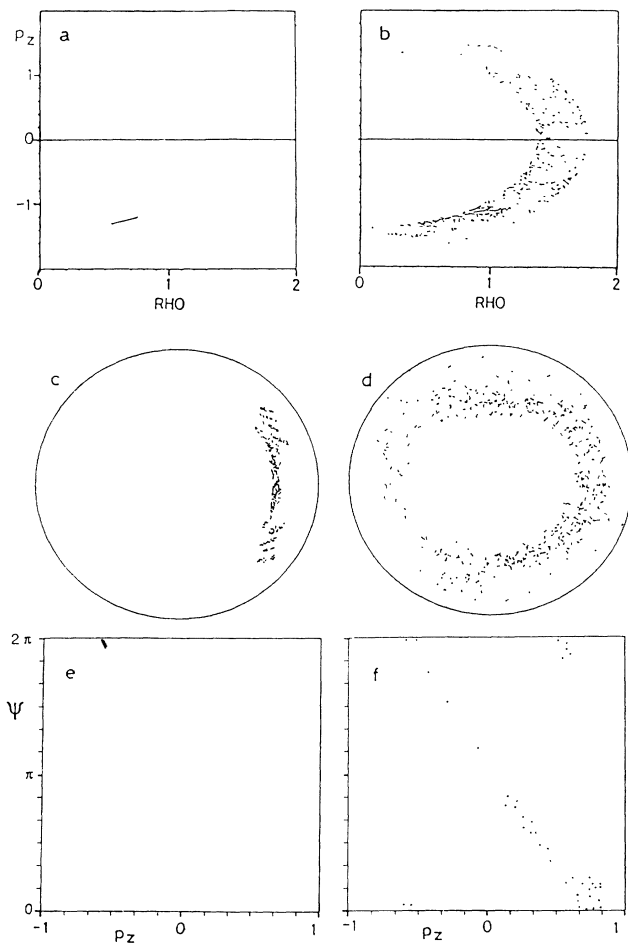


FIG. 1. (a),(c),(e) Calculated ion motion for wave amplitude below and (b), (d), (f) above threshold. Poincaré sections are shown in (a),(b) momentum space, (c),(d) configuration space, and (e),(f) a mixed space.  $\psi$  is the azimuthal angle subtended by the particle about the wave symmetry axis, it differs slightly from the guiding center coordinate  $\theta$ . Mass, length, and time are normalized to  $m$ ,  $k_{\parallel}^{-1}$ , and  $\Omega^{-1}$ .

Conservation of  $H$  during chaotic motion is illustrated in Fig 1(b). The arc  $\frac{1}{2} m P_z^2 + \frac{1}{2} m \Omega^2 \rho^2$  corresponds to the particle kinetic energy in the wave frame. A finite width is observed to this arc because of the contribution of the potential energy of the wave. An important consequence of the conservation of  $H$  is that, in the laboratory frame, chaos will change  $P_z$  primarily in the direction of wave travel provided that the particle initial perpendicular velocity is less than the wave parallel phase velocity. In the velocity plane, the particle motion is restricted to lie on arcs centered on the wave parallel phase velocity.

For a group of particles with the initial conditions shown in Fig. 1(c), conservation of  $R$  (angular momentum) results in the formation of a ring in physical space. We note that for particles off the wave axis, if the wave-particle interaction causes  $\rho$  to increase,  $R$  increases only slightly. The link between guiding center motion in the

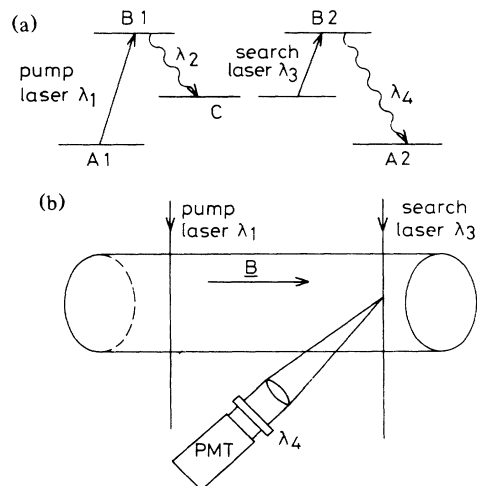


FIG. 2. Experimental configuration. (a) Fluorescence may be performed on the ground state (transition A1-B1) and on the metastable (transition C-B2). The former may be used to populate the metastable, the latter to detect it. The wavelengths in  $\text{\AA}$  are the following:  $\lambda_1=4934$ ,  $\lambda_2=6497$ ,  $\lambda_3=5854$ ,  $\lambda_4=4554$ . (b) A pump beam is used to create metastable test particles and a search beam, on a movable carriage, is used to detect them.

$\hat{E} \times \hat{B} = \hat{\theta}$  direction and parallel acceleration implied by Eq. (2) is shown in Fig. 1(f). Note that in Fig. 1, we plot the particle position  $(\psi, r)$  which differs slightly from the guiding center position  $(\theta, R)$ , but is what we measure experimentally. Each of the three conservation laws of the wave-particle Hamiltonian has the effect of constraining the phase-space excursion of particles even during chaotic motion.

Experimental observations of wave-particle interactions, of the type described above, are performed at the Alfred P. Sloan Laboratory for Mathematics and Physics  $Q$  machine with use of barium plasma and capacitively coupled electrostatic ion cyclotron waves.<sup>4</sup> The plasma is a 475-cm length, 5-cm-diam cylinder in a uniform magnetic field  $B \leq 0.3$  T. Temperatures of  $T_e \sim T_i \sim 0.15$  eV and densities of  $n_e \sim 10^9 \text{ cm}^{-3}$  are typical. Low-density barium  $Q$  plasmas are ideal for studies of collisionless plasma physics because the ionic spectrum permits extensive use of laser-induced fluorescence diagnostics on the ions with visible radiation.<sup>5</sup>

The experimental setup and ionic transitions used are shown in Fig. 2. Laser-induced fluorescence yields a measure of the ion velocity distribution function, along the laser beam, which is resolved in space and time.<sup>6</sup> The distribution function parallel to the magnetic field is measured by introducing the laser beam through a fine mesh at the end plate. Because barium ions have long-lived ( $\sim 1$  sec) metastable states, "test particles" can be created by selective optical pumping. An ion in a metastable state [C in Fig. 2(a)], though it has the same charge and mass, is easily distinguished because it will

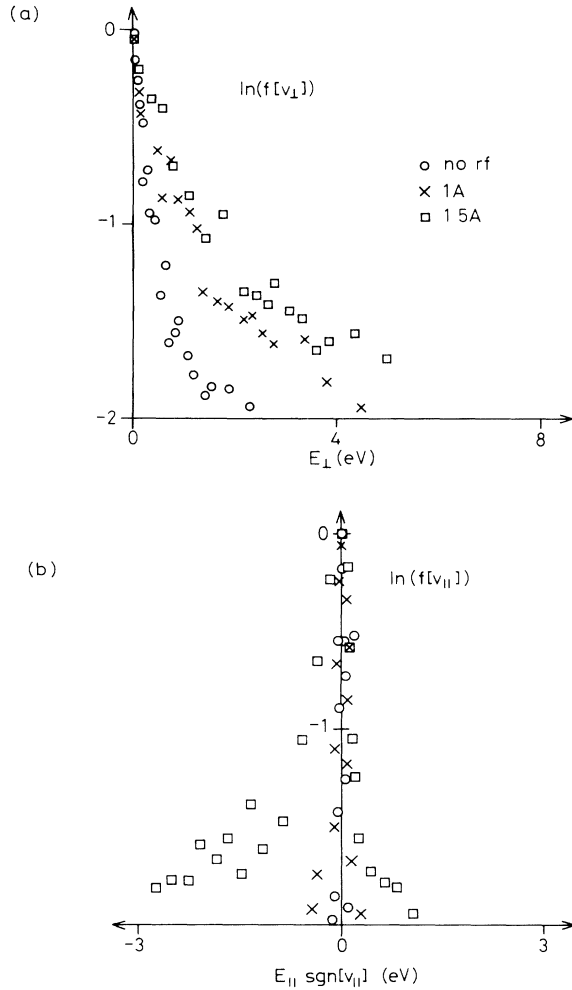


FIG. 3. Ion distribution functions as a function of antenna current (wave amplitude). 1.5 A corresponds to  $k_{\perp}^2 e \Phi / m \Omega^2 \sim 0.2$ . (a) Perpendicular energy distribution and (b) parallel energy distribution.

fluoresce on different transitions than will an ion in the ground state. The creation of metastable test particles by optical pumping provides a way to follow ion trajectories in phase space.<sup>7</sup> For these experiments, a pulsed laser is used to quickly ( $\sim 10$  nsec) create metastable particles along a vertical chord at a given axial position, and a cw laser beam on a movable carriage is used to detect test particles as a function of position, time, and velocity [Fig. 2(b)].

Propagating electrostatic ion cyclotron waves are launched from an insulated capacitor plate antennae.<sup>4</sup> The dispersion relation is measured with probes as well as through laser measurements of the linear perturbation of the ion distribution function.<sup>8</sup> Stochastic heating of plasma ions is observed when the wave amplitude is sufficient to exceed the stochasticity threshold.<sup>3</sup> In earlier experiments, measurements were made of the ion velocity distribution functions perpendicular to the mag-

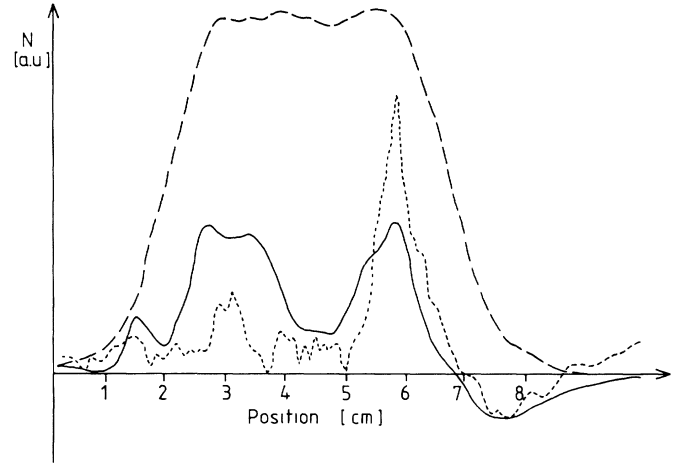


FIG. 4. Density profiles on a horizontal chord. Long-dashed curve indicates electron density. Test particle density ( $\times 10$ ) is given by the short-dashed curve (below threshold) and the solid curve (above threshold).

netic field.<sup>2</sup>

Measurements of the ion distribution function in barium plasma (Fig. 3) indicate the threshold of Smith and Kaufman for accelerations of plasma ions parallel to the magnetic field.<sup>3</sup> Broadening of the perpendicular distribution function shown in Fig. 3(a) is seen at a slightly lower wave amplitude (antenna current). In Fig. 3(b) there is evidence for the conservation of the first of the three integrals mentioned above; the particle energy in the wave frame ( $H$ ). Parallel to  $B$ , particles are accelerated primarily in the direction of wave travel ( $-Z$ ). Furthermore, particle acceleration along arcs in velocity space centered on the wave parallel phase velocity ( $\sim 1.8 \times 10^5$  cm/sec) is consistent with the range of energies observed in Fig. 3(b) ( $\epsilon < 4.5$  eV).

Information on the spatial excursions of particles is necessary in order to test the conservation of  $R$ . With a pulsed dye laser to create an off-axis vertical chord of test particles, the distribution of subsequent particle positions is investigated with a cw search laser. The volume interrogated by the search laser, defined by the intersection of the search beam and the viewing volume of the detector telescope, is scanned along a horizontal chord which passes through the plasma symmetry axis (which is also the wave symmetry axis). Figure 4 shows the results from such a scan both below and above the stochasticity threshold. Below threshold, particles move along the straight field lines. The long-dashed curve in Fig. 4 is the plasma electron density profile. Short dashes are used on the same figure to indicate the excess metastable density profile at a distance of 27 cm (sensitivity  $\times 10$ ) produced by the pump laser in the presence of a low amplitude wave whose amplitude does not exceed the threshold for chaotic acceleration.

Finally, the excursions of the guiding centers in the  $\theta$

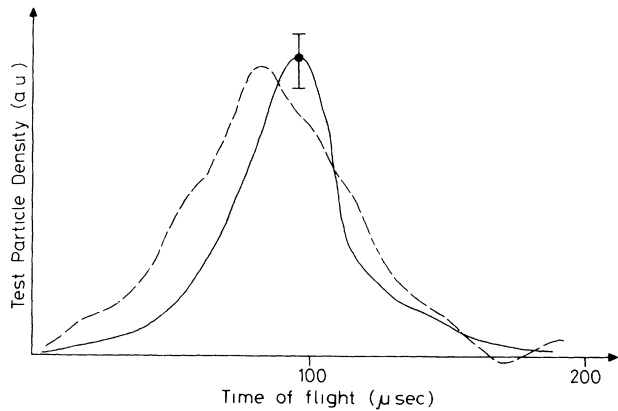


FIG. 5. Time-of-flight spectra (ensemble average) at  $R = 1.5$  cm and  $\psi = 0$  (solid curve),  $\psi = \pi$  (dashed curve).

direction should be linked to changes in parallel velocity. Thus, a change in  $\theta$  of  $\pi$  rad should be correlated with a change in  $P_Z$  given approximately by the following:

$$\Delta P_Z = (k_{\parallel}/k_{\perp}) m \Omega R \pi.$$

A nearly linear relationship is seen in Fig. 1(f) which agrees with this formula. Experimentally, this correlation is most easily seen through changes in the time of flight of test particles as they move between the pump and search laser beams. Although the motion is chaotic, the parallel velocity is not unbounded and, given the net  $\Delta P_Z$  for a particle, the change in time of flight can be approximated by the following:

$$\Delta t \sim \Delta Z / V_D - \Delta Z / [V_D + \frac{1}{2} \Delta P_Z / m],$$

where  $V_D$  is the nominal parallel drift of the  $Q$  plasma.<sup>5</sup> Using  $\Delta\theta = \pi$ , one obtains  $\Delta t \sim 20 \mu\text{sec}$ . Figure 5 shows two time-of-flight spectra at diametrically opposed points on the horizontal chord. Those which remain at  $\Psi \sim 0$  (see definition in Fig. 1 caption) have a longer time of flight, on the average, than those which have been transported to  $\Psi \sim \pi$ . The peaks of these spectra are separated by the  $20 \mu\text{sec}$  predicted above.

Each of the three measurements presented above argue for the conservation of  $H$ ,  $R$ , and  $P_Z - (k_{\parallel}/k_{\perp}) m \Omega R \theta$ , respectively. Despite the broadening of the distribution function which results from exceeding the stochasticity threshold, the individual particle motions continue to observe the basic symmetries of the wave-particle interaction Hamiltonian. Chaos during wave-particle interaction is seen to produce rapid, though constrained, transport of particles in coordinate space as well as in velocity space.

We express our appreciation to Dr. H Van den Bergh of the Swiss Federal Institute of Technology, Lausanne, and to Spectra Physics for lending us laser components. This work was partially funded by the Swiss National Science Foundation under Grants No. 2.868-0.85 and No. 2.869-0.85, and by the U.S. National Science Foundation under Grant No. INT-840.5076.

<sup>(a)</sup>Permanent address: University of California, Irvine, CA 92717.

<sup>(b)</sup>Permanent address: University of Colorado, Boulder, CO 80309.

<sup>1</sup>A. J. Lichtenberg and M. A. Lieberman, *Regular and Stochastic Motion* (Springer-Verlag, New York, 1983), p. 300.

<sup>2</sup>F. Skiff, F. Andereg, and M. Q. Tran, *Phys. Rev. Lett.* **58**, 1430 (1987).

<sup>3</sup>G. R. Smith and A. N. Kaufman, *Phys. Rev. Lett.* **34**, 1613 (1975).

<sup>4</sup>F. Skiff, F. Andereg, M. Q. Tran, P. J. Paris, T. N. Good, R. A. Stern, and N. Tynn, in *Proceedings of the Second International Conference on Plasma Physics, Kiev, U.S.S.R., 1987* (Naukova Dumka, Kiev, 1987), Vol. 1, p. 55, and in *Plasma Physics, Proceedings of the Invited Papers*, edited by A. Sitenko (World Scientific, Singapore, 1987), Vol. 1, p. 441.

<sup>5</sup>D. N. Hill, S. Fornaca, and M. G. Wickham, *Rev. Sci. Instrum.* **54**, 309 (1983).

<sup>6</sup>R. A. Stern and J. A. Johnson, III, *Phys. Rev. Lett.* **34**, 1548 (1975).

<sup>7</sup>R. A. Stern, D. N. Hill, and N. Rynn, *Phys. Lett.* **93A**, 127 (1983).

<sup>8</sup>F. Skiff and F. Andereg, *Phys. Rev. Lett.* **59**, 896 (1987).